Improved ''Optical Highlighter'' Probes Derived from Discosoma Red Fluorescent Protein

Lisbeth C. Robinson and Jonathan S. Marchant
Department of Pharmacology, University of Minnesota Medical School, Minneapolis, Minnesota

ABSTRACT The tetrameric red fluorescent protein, DsRed, undergoes a rapid red to green color change evoked by short wavelength ($\lambda < 760$ nm) femtosecond irradiation—a phenomenon that underpins the application of DsRed as an "optical highlighter" probe for tracking live cells, organelles, and fusion proteins. This color change results from selective bleaching of the "mature" red-emitting species of DsRed and an enhancement of emission from the "immature" green species, likely caused by dequenching of fluorescence resonance energy transfer occurring within the protein tetramer. Here, we have examined the role of residues known to influence the rate and completeness of chromophore maturation on the cellular and biophysical properties of DsRed mutants. Surprisingly, a single amino acid mutation (N42Q) with increased basal green emission yet rapid chromophore maturation displayed a multiphoton-evoked color change that was brighter, more consistent, more vivid, and easier to evoke than DsRed, despite the larger proportion of green chromophores. Rapidly maturing mutants with more complete chromophore maturation, exhibited little color change and increased resistance to multiphoton bleaching. We describe improved optical and cell biological properties for two DsRed-derived variants which we showcase in photolabeling studies, and discuss these data in terms of implications for fluorescence resonance energy transfer-based probes.

INTRODUCTION

The application of fluorescent proteins as expression markers and protein fusion partners has proved immensely valuable for resolving the organization of biological events in living cells, tissues, and organisms (Hadjantonakis et al., 2003; Lippincott-Schwartz et al., 2001; Verkhusha and Lukyanov, 2004). As the discovery of novel fluorescent protein variants has accelerated (Labas et al., 2002; Matz et al., 2002; Miyawaki, 2002), and the properties of these natural products have been ingeniously modified in the laboratory (Campbell et al., 2002), the expanding repertoire of biophotonic tools has allowed many live-cell experimental analyses previously regarded as infeasible.

One area of recent progress concerns the development of optical marking methods used to differentially highlight cells, organelles, and fusion proteins for tracking purposes. Such methods have found utility for studying organelle dynamics, protein trafficking, and cell lineage, as well as for selective retrieval of marked cells from within a population. Practically, optical marking strategies amenable for application in live cells depend upon rapid, light-induced changes in the emission spectrum of fluorescent protein probes. This has been achieved either by stimulating fluorescence emission from a poorly-fluorescent precursor (e.g., ''photoactivation'' or ''kindling'' (Chudakov et al., 2003; Lippincott-Schwartz et al., 2003; Patterson and Lippincott-Schwartz, 2002)), or by evoking a clearly distinguishable color change in the fluorescent protein emission spectrum (e.g., from red to green or vice versa (Ando et al., 2002; Marchant et al., 2001)). Both these strategies represent ''second-generation'' tools for tracking applications, in the sense that they can be used to directly track objects of interest after photolabeling, rather than indirectly monitor movement via fluorescence recovery into a photobleached region as with traditional fluorescence recovery after photobleaching-based approaches. However, irrespective of mechanism, the desired properties of these optical markers for live-cell applications are identical—ideally maximizing the extent, duration, and practical ease of evoking the change, while minimizing the toxicity of the probe and the labeling process to cells. Each of the currently available optical markers possesses discrete advantages and disadvantages in this regard, and there is an ongoing need to refine the properties of these lead probes further.

For example, the widely employed anthozoan red fluorescent protein drFP583 (commercially available as DsRed (Matz et al., 1999)) can be utilized as an ''optical highlighter'' in live mammalian cells (Marchant et al., 2001). Multiphoton excitation of DsRed at short wavelengths evokes a vivid and rapid color change in DsRed fluorescence emission from a red to green species (λ change ~80 nm), when viewed by regular epifluorescence microscopy. The multiphoton-evoked ''greening'' method can be used to label entire cells expressing soluble DsRed protein, but moreover the tight focality of multiphoton excitation permits optical labeling of defined subcellular regions and fusion proteins restricted within discrete organelles (Marchant et al., 2001). This color change occurs as a serendipitous consequence of the structure of DsRed, which naturally exists as an obligate tetramer containing four fluorophores that take several days to ''ripen'', passing through a phase dominated by a green fluorescent intermediate (excitation 475–485 nm,

Submitted May 7, 2004, and accepted for publication November 5, 2004.

Address reprint requests to Lisbeth C. Robinson, Dept. of Pharmacology, University of Minnesota, Minneapolis, MN 55455. Tel.: 612-624-6687; Fax: 612-625-8408; E-mail: robi0386@tc.umn.edu.

0006-3495/05/02/1444/14 $2.00

doi: 10.1529/biophysj.104.045617

emission ~500 nm) before the generation of the red-emitting protein (Baird et al., 2000; Verkhusha et al., 2004; Wall et al., 2000; Yarbrough et al., 2001). Since the maturation process is incomplete, fluorescence-resonance energy transfer (FRET) occurs between the green- and red-emitting species in ''mature'' heterooligomers (Baird et al., 2000; Cotlet et al., 2001; Heikal et al., 2000; Lounis et al., 2001; Wall et al., 2000), such that blue excitation results in a weak-green, but a strong-red emission. Multiphoton excitation ($\lambda < 760$ nm) selectively bleaches the mature, red-emitting species, enhancing the green fluorescence emission through dequenching of the intrinsic FRET (Marchant et al., 2001). Although the native DsRed protein suffices as a photolabeling tool, a key modification that would improve its utility as a probe would be to lessen the variability in the magnitude of the observed color change. Several factors contribute to this variability including the protracted timecourse and variable completeness of the chromophore maturation process as well as the tendency of the protein to oligomerize into aggregates that are resistant to the multiphoton-evoked color change. Moreover, the extent of color change (~2.4-fold enhancement in green fluorescence, ~90% reduction in red fluorescence) could be further maximized in variants exhibiting either a higher number of monomers involved in FRET or higher FRET efficiency between the green and red fluorophores—properties which would be expected to be manifest in a subset of variants with decreased basal green emission. For these reasons, we have investigated the relationship between chromophore maturation kinetics and the utility of these DsRed-derived mutants for use as optical highlighters. Here, we have identified two red fluorescent protein (RFP) variants with considerably improved optical and cell biological properties over the parent DsRed protein, which we showcase as optical highlighters in subcellular labeling studies. Our data demonstrate that modification of residues that speed maturation does not abrogate the multiphoton-evoked red-to-green color change, provided that the maturation process remains incomplete for a proportion of the fluorophores. Surprisingly, for these tetrameric probes, the elevated basal green emission does not necessarily reduce the extent of the FRET-based color change. Rapidly maturing mutants with more complete chromophore maturation, exhibited little color change and increased resistance to multiphoton bleaching. Therefore, the kinetics of chromophore maturation—both the rate and extent of this process—dictate the usefulness of RFP variants as optical highlighters.

MATERIALS AND METHODS

Vector subcloning of RFP variants

Five RFP variants derived from DsRed were used in this study: DsRed[N42Q] (Bevis and Glick, 2002), DsRed[R2A, K5E, K9T, V105A, I161T, S197A] (DsRed-2 (Yanushevich et al., 2002)), DsRed[R2A, K5E, N6D, T21S, H41T, N42Q, V44A, C117S, T217A] (DsRed-T1 (Bevis and Glick, 2002)), DsRed[R2A, K5E, N6D, T21S, H41T, N42Q, V44A, A145P] (DsRed-T3 (Bevis and Glick, 2002)), and a monomeric RFP (mRFP-1 (Campbell et al., 2002)). Each of these six RFPs (DsRed, DsRed[N42Q], DsRed-2, DsRed-T1, DsRed-T3, and mRFP-1) were subcloned into mammalian expression vectors containing the cytomegalovirus (CMV) promoter. DsRed[N42Q] and DsRed-T3 (Bevis and Glick, 2002) were excised from pQE31 using *Hin*dIII and *Bam*HI and subcloned into pCMV-Tag3A (Promega, Madison, WI). mRFP-1 (Campbell et al., 2002) was released from pRSET-B by double digestion using *Bam*HI and *Eco*RI and subsequently ligated into pCMV-Tag3A. DsRed-T1 (also known as ''DsRed Express''), DsRed, and DsRed-2 are commercially available from BD Biosciences (Palo Alto, CA). DsRed[N42Q] was targeted to mitochondria by ligating the *Bam*H1/*Hin*dIII excision fragment from pQE31 together with the *Hin*dIII/*Not*I fragment from pcDNA3.1 (Invitrogen, Carlsbad, CA) into *Bam*HI and *Not*I digested pDsRed2-mito (BD Biosciences, Palo Alto, CA). DsRed-2-ER comprises a fusion of DsRed-2 with endoplasmic reticulum targeting and retention sequences (BD Biosciences). For purification of RFP variants from bacterial cultures, BL21(D3E) cells were transformed and cultured at 37°C for 75 h as previously described (Mizuno et al., 2001). Fluorescent protein was recovered from media, concentrated using Centriprep YM-30 centrifugal filter devices (Millipore, Billerica, MA), and cell lysate by hydrophobic interaction chromatography using Econo-Pac t-Butyl HIC cartridges (Bio-Rad, Hercules, CA). The elution was further purified by gel exclusion chromatography in G-150 Sephadex (Pharmacia, Basking Ridge, NJ) columns with 10 mM Tris, pH 8.8, running buffer.

Cell culture and RFP expression

HEK-293 cells (ATCC, CRL-1573) were grown (37°C, 5% CO_2) on poly-D-lysine-coated glass-bottomed Petri dishes (MatTek Corp., Ashland, MA) in mineral essential medium supplemented with 10% horse serum. Monolayers were transfected at ~70% confluency with individual constructs using Lipofectamine-2000 reagent (Invitrogen) and incubated for an additional 24–48 h before imaging. Cells were washed with HEPES-buffered medium (NaCl 135 mM, KCl 5.9 mM, $CaCl_2$ 1.5 mM, $MgCl_2$ 1.2 mM, HEPES 11.6 mM, glucose 11.5 mM, pH 7.3) and sealed within a leak-proof imaging chamber to allow use of oil-immersion objective lenses. HT-1080 human fibrosarcoma cells (ATCC, CCL-121) were cultured in Dulbecco's modified Eagle's medium with 10% fetal bovine serum and transfected as described above.

Spectroscopic studies and cellular imaging

Fluorescence imaging was performed using an Olympus B-Max 50WI upright microscope equipped with a standard epifluorescence system (100 mW mercury arc lamp) and a Bio-Rad MRC1024ES scanning confocal module for single photon ($\lambda = 488$ nm) and multiphoton *xy* imaging (Tsunami, Spectra-Physics, Mountain View, CA). Fluorescence spectra were collected from individual cells using a C-mounted spectrophotometer and field aperture (USB2000, Ocean Optics, Dunedin, FL) using a standard fluorescein isothiocyanate (FITC) cube (MWIB, excitation 460 ± 90 nm, 505 nm dichroic, emission >515 nm) and tetramethylrhodamine isothiocyanate cube (MWIG, excitation 535 ± 15 nm, 565 nm dichroic, emission >580 nm). For better quantification of the green-emitting species by epifluorescence excitation, a Piston green fluorescent protein (GFP) filter set with a 515 ± 15 nm band-pass emission filter was used (#41025, Chroma Technology, Rockingham, VT). For quantification of fluorescence by confocal excitation, fluorescence excited by the 488-nm line of an argon ion laser was emission-filtered (green, $\lambda = 522 \pm 17$ nm; red, $\lambda > 585$ nm) before detection via separate photomultiplier tubes. Fluorescent quantum yields were determined according to cross-comparative methods (Williams et al., 1983), using equally absorbing standards of rhodamine B and rhodamine 101 in ethanol ($\lambda_{EX} = 535$ nm, integrated fluorescence emission between 550 and 800 nm). Excitation spectra were acquired at $\lambda_{EM} = 600$ nm from a partially purified lysate of transfected HEK-293 cells (treated with

M-Per Reagent (Pierce, Rockford, IL)) using an ISS K2 Multiphase Fluorometer (ISS, Champaign, IL).

Flow cytometry

Monolayers of HEK-293 cells were transfected within T25 tissue culture flasks using ~2 μg of cDNA of individual fluorescent protein variants. HEK-293 cells were used for these experiments because their high transfection efficiency (~75% [DsRed-1, DsRed-N42Q], 87% [DsRed2]) permitted measurements from large populations of positively transfected cells (>20,000). Cells were trypsinized and resuspended in Ca^{2+}-free phosphate-buffered saline (KCl 2.67 mM, KH_2PO_4 1.5 mM, NaCl 138 mM, Na_2HPO_4 8 mM) and populations screened using a FACS-Calibur machine (BD Immunocytometry Systems, San Jose, CA (Marchant et al., 2002)) for the proportion of positively transfected cells (a crude index of cell tolerance to expression of individual RFPs), as well as the average population intensity of fluorescence emission (an index of relative brightness of individual variants when expressed in live cells, useful for comparison to measured quantum yields measured in vitro).

RESULTS

For these experiments, we selected five RFP variants derived in the laboratory by mutagenesis of DsRed (DsRed[N42Q], DsRed-2, DsRed-T1, DsRed-T3, and mRFP-1). Four of

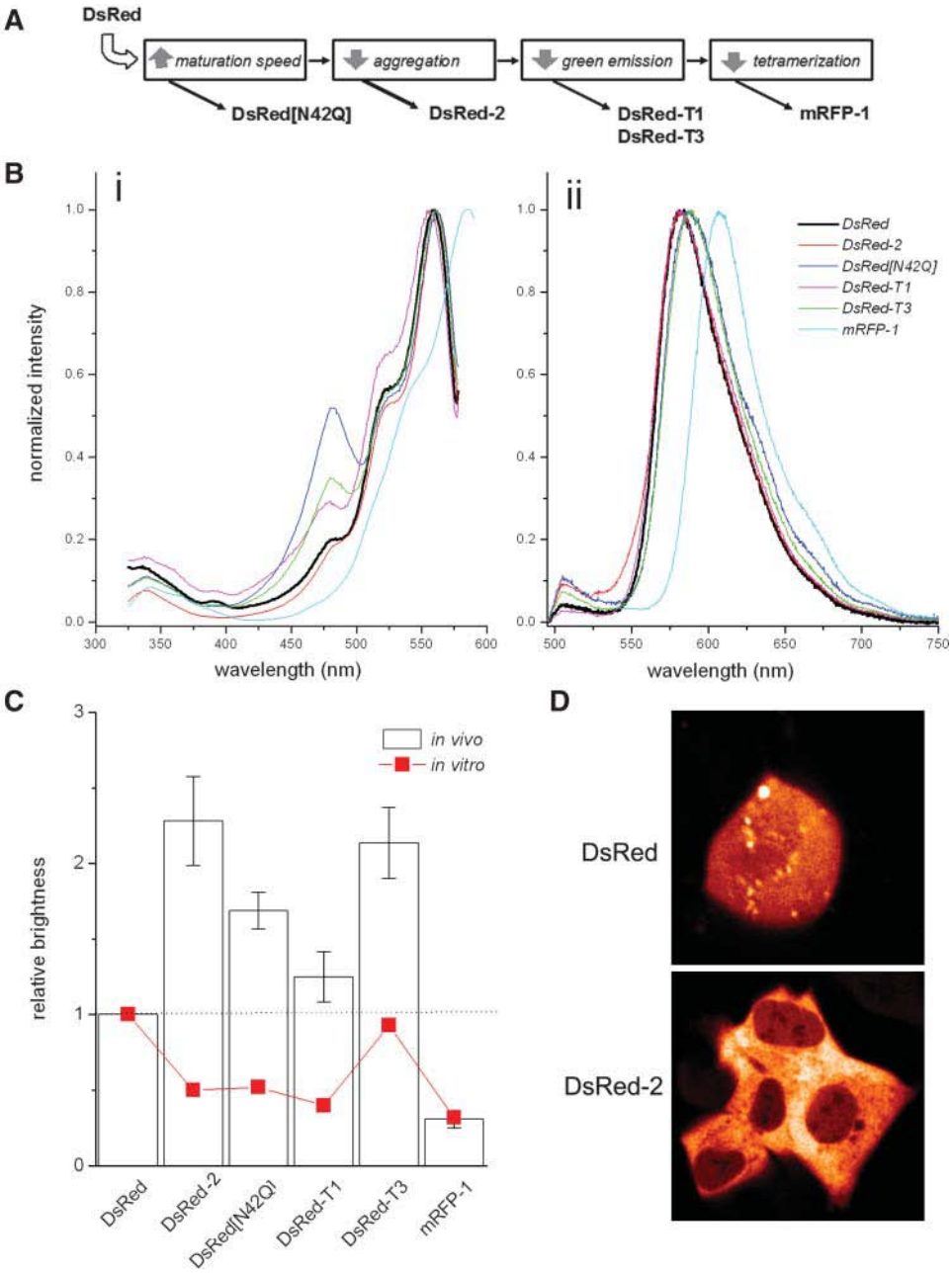

FIGURE 1 Basic properties of RFP variants. (*A*) Scheme to illustrate the interrelationship between the DsRed-derived variants in terms of the functional effect of introduced amino acid changes. For example, in relation to DsRed, DsRed-T1 contains amino acid substitutions that speed maturation, decrease aggregation, and decrease green emission. (*B*) Normalized (*i*) excitation and (*ii*) emission spectra of RFP variants. For excitation spectra, emission was monitored at 600 nm. For emission spectra, cells were excited with epifluorescence illumination using a Piston GFP cube and/or a standard FITC filter cube (λ_{EX} = 460 ± 90 nm, 505 nm dichroic, λ_{EM} > 515 nm). (*C*) Relative intensity of variants compared in vitro (*bars*) and within transfected cells (in vivo, *squares*) to illustrate the different rank order of the brightness of probes observed in cells compared to purified samples. The in vitro brightness is approximated as the product of quantum yield and extinction coefficient expressed relative to DsRed. For in vivo measurements, flow cytometry analysis was used to measure mean population fluorescence of positively transfected cells (λ_{EX} = 488 nm, λ_{EM} = 585 ± 21 nm). HEK-293 cells were transfected ~48 h previously with equal amounts of cDNA encoding individual RFP variants. Data are normalized relative to data with DsRed. (*D*) Confocal images of HEK-293 cells expressing either DsRed (*top*) or DsRed-2 (*bottom*) illustrating the lower degree of aggregation observed with the newer RFP variants (e.g., DsRed-2). Cells were grown at 37°C and transfected with ~0.5 μg of cDNA ~48 h before imaging. Variants were excited using the 568-nm laser line and emitted fluorescence monitored with a long-pass filter (λ_{EM} > 585 nm) and represented using a standard color table.

these proteins exhibited characteristics which we hypothesized would better the performance of DsRed as an optical highlighter probe (Fig. 1 *A*). For example, DsRed[N42Q] harbors a single amino acid change, resulting in a faster—but still incomplete—maturation of red fluorescence (Bevis and Glick, 2002), which we surmised would increase the consistency of color changes observed on greening (Baird et al., 2000; Marchant et al., 2001). DsRed-2 incorporates a different set of amino acid substitutions that speed maturation (Terskikh et al., 2002), as well as a trio of additional mutations that neutralize positive charges in the NH_2-terminal region lowering the propensity of the protein to oligomerize into cellular aggregates (Yanushevich et al., 2002). Decreasing the formation of red aggregates, which are highly resistant to multiphoton bleaching, would potentially improve the visibility of the color change as well as cellular tolerance to overexpression of this RFP variant. The DsRed-T1 and DsRed-T3 variants contain an additional substitution that speeds maturation, a suite of NH_2-terminal substitutions to eliminate aggregation, and further mutations that reduce enhanced green emission associated with the N42Q substitution (Bevis and Glick, 2002). Reductions in green emission may indicate a variant with improved FRET efficiency, or more complete maturation (see Discussion). Finally, in an experimental tour de force of rational and random mutagenesis, Campbell et al. (2002) generated a monomeric RFP variant (mRFP-1, 33 mutational changes from DsRed-1) incorporating all of the above characteristics as well as conquering the requirement for tetramerization in the production of red fluorescence. Therefore, mRFP-1 provides useful insight for these studies, as a monomeric RFP could only be expected to exhibit a color change attributable to photoconversion rather than a FRET dequenching mechanism.

Properties of RFP variants in mammalian cells

Transient transfection of DsRed and the five RFP variants into HEK-293 cells resulted in the manifestation of an orange/red fluorescence throughout the cytoplasm after ~48 h, when viewed either via epifluorescence illumination with a standard ''blue'' FITC filter cube ($\lambda_{EX} = 460 \pm 90, \lambda_{EM} = 515$ LP) or with argon-ion laser excitation ($\lambda_{EX} = 488$ nm). The effect of the introduced mutants on the spectral properties of each variant was assessed via comparison of the excitation and emission spectra (Fig. 1 *B*, *i* and *ii*, respectively). All the tetrameric variants (DsRed-1, DsRed-2, DsRed[N42Q], DsRed-T1, and DsRed-T3) displayed a fluorescent component contributing between 475 and 485 nm to the excitation spectra (representing the green fluorescent species of DsRed), although the relative prominence of this component varied between different variants (Fig. 1 *B i*). The excitation spectrum for the monomeric mRFP-1 was red-shifted (~585 nm), and lacked a prominent peak in the ~500–510 nm region (Fig. 1 *B i*). The peak of the emission spectra of the tetrameric variants clustered between 583 and 589 nm, whereas the emission peak of mRFP-1 was red-shifted at ~605 nm (Fig. 1 *B ii*). These data are consistent with previous characterizations of individual variants (Bevis and Glick, 2002; Campbell et al., 2002; Matz et al., 1999; Mizuno et al., 2001; Terskikh et al., 2002).

Three differences between the properties of individual variants merit attention. First, the excitation and emission spectra demonstrated that the relative proportion of the green fluorescence species varied between constructs. For example, DsRed[N42Q] displayed the most prominent peak of blue excitation and green emission (13.8 ± 2.1%) relative to the parent DsRed construct (7.0 ± 2.2%), Fig. 1 *B*, and see Fig. 7 *B*. Second, the average brightness of cell populations transfected with individual variants was different, and moreover dissimilar to the relative intensities (product of quantum yield and extinction coefficient) of the very same proteins measured in vitro (Fig. 1 *C*). In vitro, all variants derived from DsRed-1 appeared less bright than DsRed-1, whereas populations of cells expressing the same variants were brighter than DsRed-expressing cells (except mRFP-1) assessed either by spectrometer or by flow cytometry (Fig. 1 *C*, and see Fig. 7 *B*). This difference is important for experimentalists employing live-cell imaging methods, as users should select variants with optimized fluorescence intensities within cells rather than in vitro. Third, we speculate that this difference between live-cell and in vitro measurements derives in part from the impact of aggregatory processes in live cells that are detrimental to cell growth/viability (Verkhusha et al., 2001). A crude index of cellular tolerance to individual variants is provided by the cellular transfection efficiency, which was lower for DsRed-1 (76.7 ± 0.7%), than nonaggregating variants (81.6 ± 0.3%). For DsRed-1, this effect likely undercuts the advantageous biophysical properties of the protein—whereas punctate aggregates were observed in cells expressing DsRed and DsRed[N42Q], aggregation was rarely observed with DsRed-2, DsRed-T1, DsRed-T3, and mRFP-1 (e.g., Fig. 1 *D*). In summary, these results suggest that each of the engineered RFP variants possesses select advantages over DsRed for live-cell imaging studies in mammalian cells (summarized in Fig. 7).

Multiphoton imaging of RFPs

To assess the susceptibility of the RFP variants to multiphoton-evoked color change (Marchant et al., 2001), we used a femtosecond infrared laser and a scanning confocal microscope to image HEK-293 cells expressing individual RFPs that were transfected ~48 h previously. Viewed with multiphoton excitation, red fluorescence emission was observed at both short ($\lambda_{EX} = 750$ nm) and longer wavelengths ($\lambda_{EX} = 950$ nm); however, whereas the intensity of the fluorescence emission was relatively stable at the longer wavelength, red fluorescence emission decayed rapidly at the shorter wavelength (e.g., *single traces* in Fig. 2 *A*). Longer wavelengths ($\lambda_{EX} = 950$ nm) are therefore more suitable for

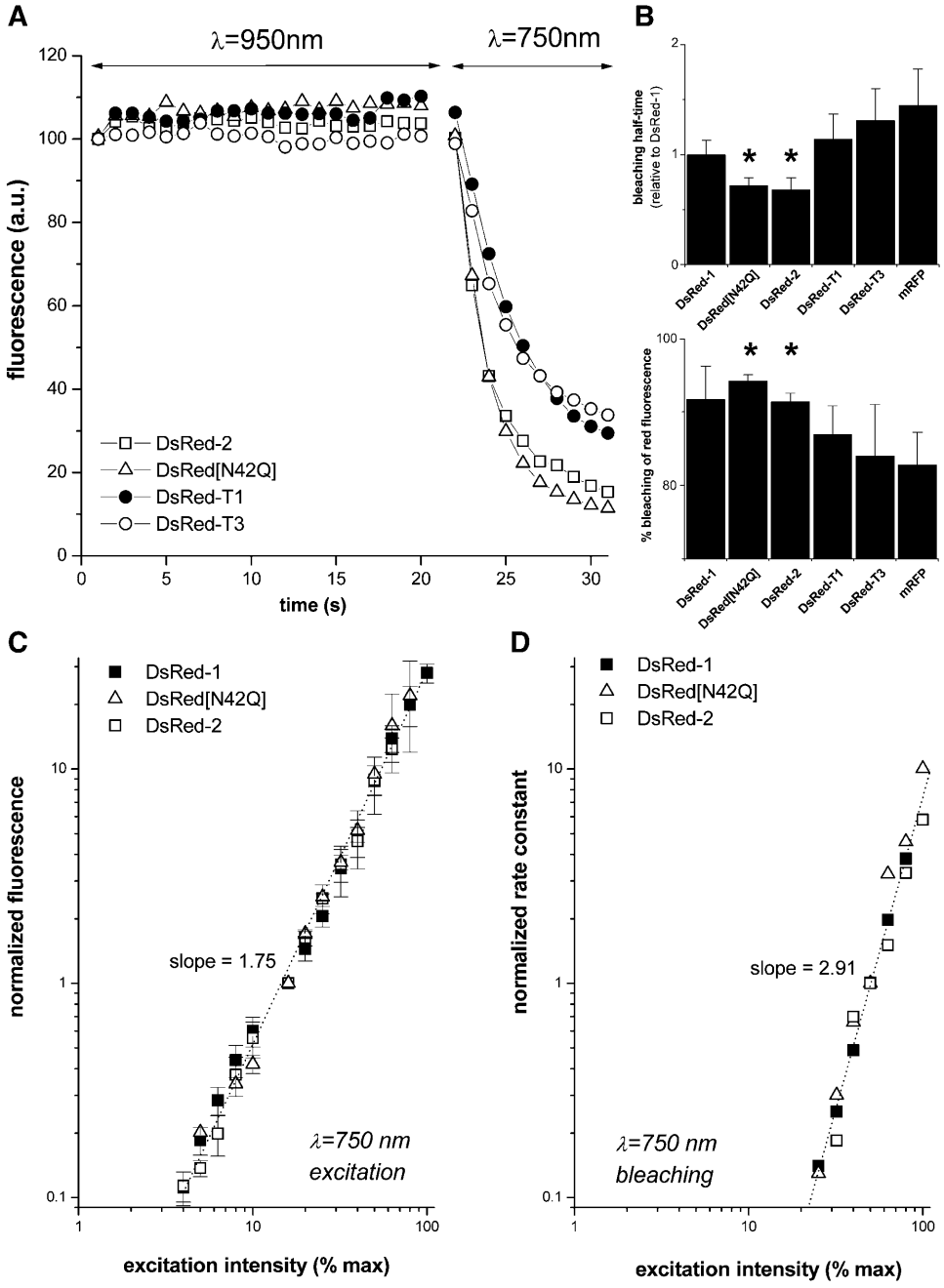

FIGURE 2 Multiphoton excitation of RFP variants and bleaching of red fluorescence. (*A*) Traces illustrating the differential stability of red fluorescence emission of DsRed variants ($\lambda_{EM} > 585$ nm) evoked by long ($\lambda_{EX} = 950$ nm) and short ($\lambda_{EX} = 750$ nm) wavelength multiphoton excitation. The intensity of laser illumination was reduced to ~16% after tuning the laser to 750 nm to attain comparable levels of fluorescence from the same specimen at $\lambda = 750$ nm and $\lambda = 950$ nm. This reduction was in part necessary to compensate for increased output from the TiSapphire laser at $\lambda = 750$ nm. (*B*) *Top*,: comparison of bleaching half-times of RFP variants after exposure to the same laser power ($\lambda_{EX} = 750$ nm). Half-times are normalized to values obtained with DsRed-1; *bottom*, comparison of the extent of bleaching of red fluorescence. Asterisks highlight the consistency of results with DsRed[N42Q] and DsRed-2 relative to the other RFP variants. (*C*) Power-law dependence for fluorescence emission from RFP variants at $\lambda_{EX} = 750$ nm. For ease of presentation, only data points from DsRed, DsRed[N42Q], and DsRed-2 are shown; data for other variants are presented in Fig. 6 *B*. The slope of the regression line for DsRed is shown, which on double logarithmic coordinates corresponds to the power function ($y \alpha x^a$) by which fluorescence increases with laser intensity. (*D*) Double-logarithmic plot to show the relative rate constants describing the decrease in fluorescence intensity of DsRed, DsRed[N42Q], and DsRed-2, where each point is derived from single-exponential fits to the profile of the decrease in fluorescence intensity at different laser powers.

imaging DsRed-derived variants by multiphoton microscopy—a result consistent with the spectral properties of the parent molecule, DsRed-1 (Hess et al., 2003; Jakobs et al., 2000; Marchant et al., 2001).

From these experiments, it was evident that both the rate and extent of the decrease in fluorescence intensity at $\lambda_{EX} = 750$ nm varied between different RFP variants. For example, whereas DsRed[N42Q] and DsRed-2 bleached more rapidly than DsRed at equivalent laser powers, the half-time for bleaching of red fluorescence was longer for DsRed-T1, DsRed-T3, and mRFP-1 (Fig. 2 *B*, *top*). This increased resistance to multiphoton photobleaching was not due to the use of a nonoptimal wavelength for bleaching different variants, as this disparity was maintained across a range of wavelengths (730–750 nm) over which DsRed is susceptible to multiphoton-evoked bleaching (data not shown). Furthermore, the red fluorescence of DsRed[N42Q] and DsRed-2 bleached both more completely and more consistently than any of the other variants (Fig. 2 *B*, *lower*). Estimation of the power function for excitation and for the rate of bleaching of red fluorescence emission at $\lambda_{EX} = 750$ nm revealed that the fluorescence emission increased with approximately the

second power of laser intensity (Fig. 2 *C*, and see Fig. 7 *B*; DsRed, 1.68 ± 0.12; DsRed[N42Q], 1.64 ± 0.29; DsRed-2, 1.65 ± 0.12; DsRed-T1, 1.59 ± 0.22; DsRed-T3, 1.63 ± 0.14, $\underline{n} \geq 4$), whereas the rate constant describing the decrease in fluorescence intensity increased as a third-power function (Fig. 2 *D*, and see Fig. 7 *B*; DsRed, 2.98 ± 0.10; DsRed[N42Q], 3.05 ± 0.57; DsRed-2, 2.69 ± 0.16; DsRed-T1, $n = 3$). The less-than-quadratic dependency (<2) of the power coefficient for excitation observed at $\lambda = 750$ nm is likely attributable to rapid photobleaching (Marchant et al., 2001). At longer wavelengths (e.g., $\lambda = 920$ nm), where photobleaching is less rapid, the red fluorescence emission increases with an expected quadratic dependence on excitation intensity (e.g., DsRed, 1.96 ± 0.08; DsRed[N42Q], 1.94 ± 0.13). These data suggest that whereas fluorescence excitation at $\lambda_{EX} = 750$ nm involves two-photon absorption, the fluorescence bleaching process requires three-photon absorption (Hess et al., 2003; Marchant et al., 2001). In contrast to the rapid (seconds) photobleaching achieved using multiphoton excitation, long exposure times to intense orange one-photon excitation (>10 min from an arc lamp, 570 nm dichroic) were required to bleach the red fluorescence of DsRed variants (data not shown).

Greening of DsRed visualized by confocal microscopy

Previously, the greening effect has been demonstrated by comparison of conventional (one-photon) epifluorescence images (Fig. 3 *A*). Here, to assess the utility of this optical-marking method for use with higher resolution imaging methods (e.g., confocal microscopy) or with multiple laser-based instrumentation (e.g., flow cytometers), we used an argon-ion laser ($\lambda_{EX} = 488$ nm) to visualize multiphoton-evoked changes in the emission properties of DsRed. DsRed-expressing cells excited with a 488-nm laser exhibited little green fluorescence emission relative to the intensity of red fluorescence before exposure to the multiphoton beam. However, after multiphoton exposure ($\lambda_{EX} = 750$ nm for ~10 s), cells appeared green via subsequent argon-ion laser illumination (Fig. 3 *B i*, Supplementary Material, Movie 1). In contrast, multiphoton excitation of mRFP-1 ($\lambda_{EX} = 750$ nm) elicited a progressive photobleaching of mRFP-1 fluorescence with no accompanying color change (Fig. 3 *B ii*, Supplementary Material, Movie 2). Fig. 3 *C* depicts the timecourse of the fluorescence changes during the greening of a single HEK-293 cell expressing DsRed. Maximal enhancement of green fluorescence was achieved after <5 s, although continued bleaching of the red fluorescence improved the visibility of the color change (after 10 s, red fluorescence emission was decreased by ~90% and green fluorescence increased 2.7-fold). Consequently, the contribution of green fluorescence to the total fluorescence increased from ~3% to ~60% after multiphoton illumination (Fig. 3 *C*, *inset*; >30 cells). These changes were of similar magnitude to that observed by epifluorescence (Fig. 3 *D*), underscoring that the color change can be observed equally well via either method (Fig. 3 *E*; $n \geq 8$ cells).

Variable greening of RFP variants

Similar experiments were performed to compare the utility of DsRed[N42Q], DsRed-2, DsRed-T1, and DsRed-T3 as optical highlighters. Fig. 4 shows representative images of cells expressing these individual RFP variants before and after three-photon photobleaching captured either using epifluorescence illumination (Fig. 4 *A*) or by argon-ion laser excitation (Supplementary Material, Movies 3–6). Whereas DsRed[N42Q]- and DsRed-2-expressing cells displayed a bright, vivid green fluorescence after multiphoton excitation, the appearance of cells expressing DsRed-T1 and DsRed-T3 was typically more yellowish. Occasionally, multiphoton-bleaching of DsRed-T3-expressing cells resulted in a vivid-greening effect (see Discussion); however, the most frequent phenotype was a color change that was insufficiently distinct from neighboring unbleached cells. Emission spectra from single cells before and after three-photon bleaching (e.g., Fig. 4 *B*) demonstrated that the observed change resulted from a variable enhancement in green fluorescence (DsRed[N42Q], 267 ± 40%; DsRed-2, 130 ± 15%; DsRed-T1, 412 ± 58%; DsRed-T3, 221 ± 16%; $n \geq 15$ cells, three independent transfections) and a variable degree of bleaching of the red species of different variants (residual red fluorescence, DsRed[N42Q], 5.7 ± 0.8%; DsRed-2, 8.4 ± 1.2%; DsRed-T1, 13.1 ± 4.0%; DsRed-T3, 16.0 ± 7.1%). Time-resolved experiments made using laser excitation ($\lambda_{EX} = 488$ nm; Fig. 4 *C*) were consistent with epifluorescence measurements, by demonstrating that the green fluorescence component dominated the emission of DsRed[N42Q] and DsRed-2 after short-wavelength multiphoton excitation. In contrast, the red and green emission was more comparable from cells expressing DsRed-T1 and DsRed-T3, resulting in a composite yellow coloration.

Mechanistically, the greening effect could result from either FRET dequenching (strongly favored by previous results; Baird et al., 2000; Cotlet et al., 2001; Garcia-Parajo et al., 2001; Gross et al., 2000; Lounis et al., 2001; Marchant et al., 2001; Wall et al., 2000; Yarbrough et al., 2001) or from a photoconversion of the red protein to a green species. To distinguish these possibilities for the DsRed variants that exhibited improved properties as optical highlighters (DsRed-2 and DsRed[N42Q]), we compared the degree of greening between two populations of cells (24 h posttransfection and >50 h posttransfection) that differed in the intensity of their red-fluorescence (by 10- to 15-fold). For both variants, the percentage enhancement of green fluorescence after multiphoton excitation was similar at either time (DsRed-2, 153 ± 5.6%; DsRed[N42Q], 213 ± 33%; Fig. 5, *A* and *B*), despite the substantial increases in red

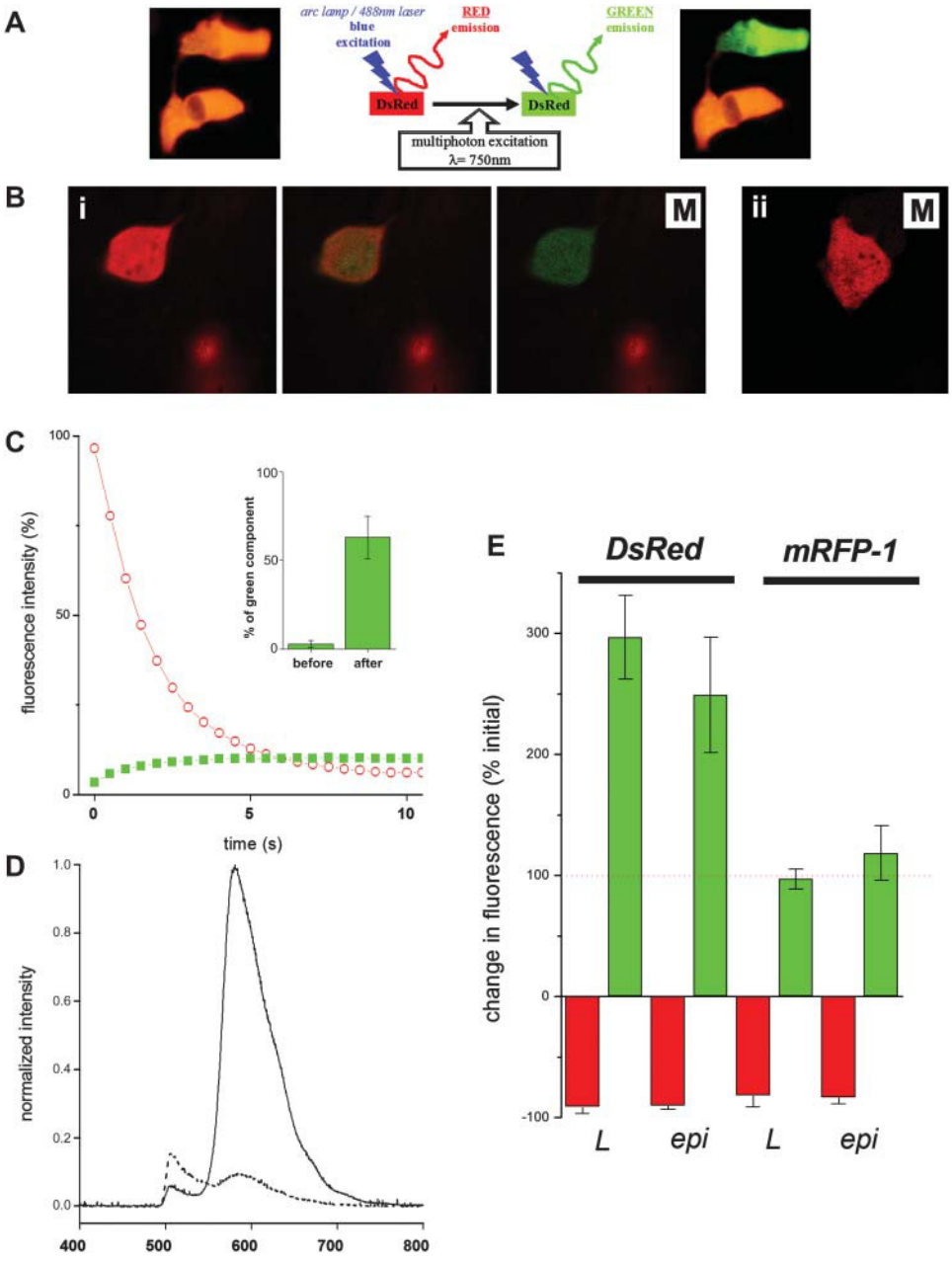

FIGURE 3 Greening of DsRed is observable by fluorescence and confocal microscopy. (*A*) Schematic illustrating the principle of the optical highlighting process. Before multiphoton excitation, DsRed-expressing cells appear orange-red by excitation with blue light (either 488 nm laser light or epifluorescence illumination). However, cells exposed to short-wavelength multiphoton excitation ($\lambda_{EX} = 750$ nm, *upper cell*) for several seconds subsequently appear green in response to the same excitation sources. (*B*) (*i*) Image planes taken from a movie (*M* denotes Movie 1 of Supplementary Material) to illustrate the change in fluorescence emission ($\lambda_{EX} = 488$ nm) from a DsRed-expressing HEK-293 cell during the multiphoton-bleaching process. To generate the composite movie, individual red and green PMT channels (green, $\lambda_{EM} = 522 \pm 17$ nm; red, $\lambda_{EM} > 585$ nm) were merged. The red spot in the lower half of each image represents an internal reflection of the multiphoton beam. (*ii*) First image plane from a movie (*M* denotes Movie 2 of Supplementary Material) which shows that the multiphoton bleaching of mRFP-1 fluorescence is not accompanied by a color change. (*C*) Representative time course of change in green and red fluorescence emission (green, $\lambda_{EM} = 522 \pm 17$ nm; red, $\lambda_{EM} > 585$ nm) during continued exposure to femtosecond laser illumination ($\lambda_{EX} = 750$ nm, ~20 $\mu W/\mu m^2$). Data are expressed relative to the percentage of red and green components in the initial fluorescence emission. (*Inset*) Contribution of green fluorescence peak to ''total'' fluorescence (green and red fluorescence peaks) before and after multiphoton laser exposure. (*D*) Greening of DsRed arises from a reduced red, but enhanced green fluorescence. Emission spectra from a single cell before (*solid line*) and after (*dashed line*) multiphoton excitation. (*E*) The magnitude of observed changes in red and green fluorescence intensity after multiphoton excitation are comparable when viewed either by argon-ion laser (*L*, $\lambda_{EX} = 488$ nm) or epifluorescence illumination (*epi*) for both DsRed (*left*) and mRFP-1 (*right*).

fluorescence emission with increasing time after transfection. Such a result would not be expected from a process attributable to photoconversion of the mature red chromophore.

Application of DsRed variants as optical highlighters for subcellular labeling

Although this greening technique can be used to optically mark entire cells expressing soluble DsRed-derived variants (e.g., Figs. 3 and 4), the tight focality of the three-photon excitation process also permits the color change to be evoked within more defined subcellular regions, for example, regions of the cytoplasm, the nucleus, or organelles expressing individual DsRed variants (Fig. 6). To demonstrate this, we constructed a DsRed[N42Q] variant targeted to mitochondria via fusion of the fluorescent protein to a mitochondrial import sequence (Fig. 6 *A i*). In cells expressing this variant, specific areas of the mitochondrial network could be greened without obvious perturbation of mitochondrial

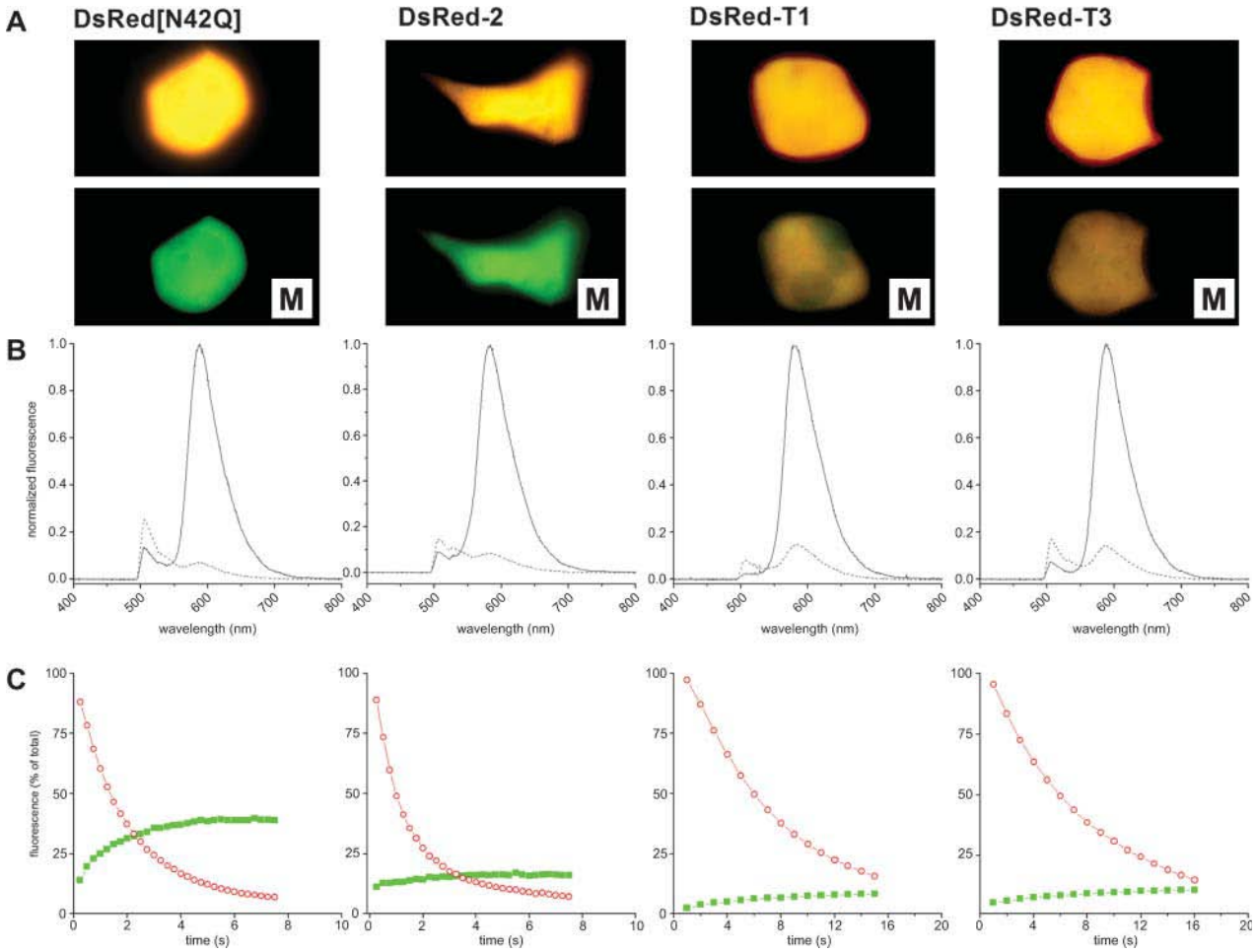

FIGURE 4 Comparison of DsRed-derived variants as optical highlighters. (*A*) Epifluorescence images of HEK-293 cells expressing individual RFP variants before (*top*) and after (*bottom*) three-photon photobleaching. Cells were chosen of similar brightness to present images of equivalent initial brightness to facilitate comparison (cf. Fig. 1 *C*). *M* denotes Movies 3–5 of Supplementary Material. (*B*) Normalized emission spectra from cells expressing individual RFP variants before (*solid line*) and after (*dashed line*) multiphoton excitation ($\lambda_{EX} = 750$ nm). Cells were excited with epifluorescence illumination using a Piston GFP filter set and a standard FITC cube. (*C*) Time course of changes in green and red fluorescence emission (green, $\lambda_{EM} = 522 \pm 17$ nm; red, $\lambda_{EM} > 585$ nm, during concurrent exposure to femtosecond laser illumination ($\lambda_{EX} = 750$ nm). Data are expressed relative to the percentage of the red and green components present in the initial fluorescence emission.

morphology (Fig. 6 *A ii*), thereby permitting discrete organelles to be subsequently tracked. The greening technique can also be applied to monitor diffusional exchange. Fig. 6 *B* shows that the cytoplasmic color gradient resulting from greening a restricted cellular region quickly equilibrated (Fig. 6 *B*) owing to free diffusional exchange of green- and red-emitting species in the cytoplasm. In contrast, diffusional exchange into nuclear lobes residing either inside or outside the multiphoton scan plane was not observed over the same time period (Fig. 6 *B*, *arrows*). Cumulative measurements of red fluorescence and green fluorescence intensity from representative diffusional exchange experiments demonstrated that the red and green fluorescent species equilibrated throughout the cytoplasm with similar kinetics (e.g., Fig. 6 *C*, *region A*), e.g., for cytoplasmic regions exposed to the multiphoton scan, the rate of influx of red-emitting species paralleled the rate of efflux of green-emitting species (half times ~7 s; Fig. 6 *C*). However, greening an area within the cytoplasm had little impact on the levels of red or green fluorescence within the nucleus over the same time period (Fig. 6 *C*, *region B*). Experiments measuring exchange rates of RFP variants expressed in different cellular compartments demonstrated that diffusional exchange was fastest in the cytoplasm (half time ~6.7 ± 4.2 s), rapid within the endoplasmic reticulum (4.9 ± 0.6 s), and slowest between the cytoplasm and the nucleus (~10 min).

DISCUSSION

DsRed displays many properties of great utility for cell biological studies. Notably, the protein exhibits a bright red, autocatalytic fluorescence emission easily separable from

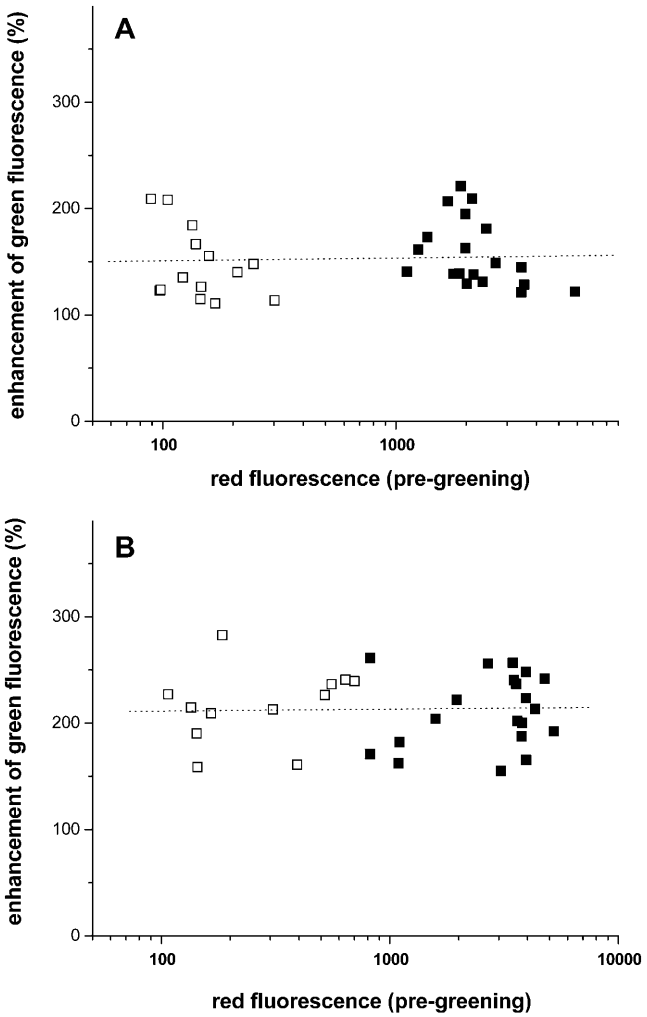

FIGURE 5 Mechanism of greening. Percentage change in green emission observed in two different populations of cells transfected either <20 h earlier (*open symbols*) or >50 h earlier (*closed symbols*) with either (*A*) DsRed-2 (early time point, 15 h) or (*B*) DsRed[N42Q] (early time point, 24 h) expressed relative to absolute red fluorescence intensity. Dashed line is a least squares fit to the entire data set.

GFP variants, as well as a high stability toward photobleaching, pH changes, and denaturation (Matz et al., 1999; Mizuno et al., 2001; Verkhusha et al., 2003). However, several properties of DsRed were quickly recognized as less than ideal for biological applications. First, the tetrameric structure of the protein and the propensity of tetramers to oligomerize further into aggregates impeded its utility as a fusion partner. Second, the complex fluorophore maturation kinetics via a green fluorescent intermediate were tardy (half-time ~1 day), incomplete, and spectrally inconvenient for multicolor labeling applications, in which cross talk with GFP-like proteins remained a problem, even after prolonged maturation (Baird et al., 2000; Gross et al., 2000; Mizuno et al., 2001). Thankfully, considerable progress has been made in deriving DsRed-based variants where the properties of residual green emission (Terskikh et al., 2002; Verkhusha et al., 2001), tetramerization (Gurskaya et al., 2001), and oligomerization (Yanushevich et al., 2002) have been tackled individually, or most impressively addressed en masse (Campbell et al., 2002). Here, however, we would stress that although the presence of the green chromophore is undesirable for certain DsRed applications and has been a target for elimination in many mutagenesis studies; it nevertheless provides an opportunity to generate useful imaging tools. First, by protracting the maturation process, DsRed[V105A,S197T] has been exploited as a convenient fluorescent timer molecule (''E5'' (Terskikh et al., 2000), commercially available as pTimer, BD Biosciences). The fluorescence of this variant gradually changes from bright green through yellow, orange, to a final red coloration and this color transition has been used to resolve the spatial and temporal patterns of promoter activity in living tissues (Terskikh et al., 2000). Second, the serendipitous discovery that multiphoton excitation ($\lambda < 760$ nm) rapidly bleaches the red species, dequenching the intrinsic FRET to result in a red-to-green color change, allows exploitation of DsRed as an optical highlighter to track cell lineage and fusion protein dynamics or to retrieve marked cells from a larger population (Marchant et al., 2001). Finally, in a zoological context, the incompleteness of the green-to-red maturation process may play an important biological role in the *Discosoma* corals where drFP583 is natively found (Matz et al., 1999), for example, coupling a photoprotective role via absorption of blue incident light to the emission of long-wavelength (red) light of utility for dinoflagellate photosynthesis (Salih et al., 2000). In short, the existence of the ''parasitic'' green fluorophore of DsRed has neglected advantages as well as clear disadvantages for discrete biological applications.

Ideal characteristics of an optical highlighter probe

For utility in tracking applications, an ideal highlighter probe should 1), be bright; 2), display a large color change after multiphoton excitation; and 3), the color change should also be easy to evoke and resolve.

Firstly, an important point for experimentalists is that the brightness of individual variants expressed in mammalian cells does not mimic measurements of fluorescence intensity made from purified proteins in vitro, as biological considerations (e.g., cell-specific toxicity, degradation, or maturation effects (Bevis and Glick, 2002; Jakobs et al., 2000; Terskikh et al., 2002)) likely impact fluorescence levels in vivo. For example, all the tetrameric variants derived from DsRed used in this study exhibited significantly brighter fluorescence on expression in live cells compared with DsRed (Fig. 1 *C ii* (BD Biosciences Clontech, 2001)), in contrast to spectroscopic studies using purified proteins (Bevis and Glick, 2002; Campbell et al., 2002). This may partly result from the

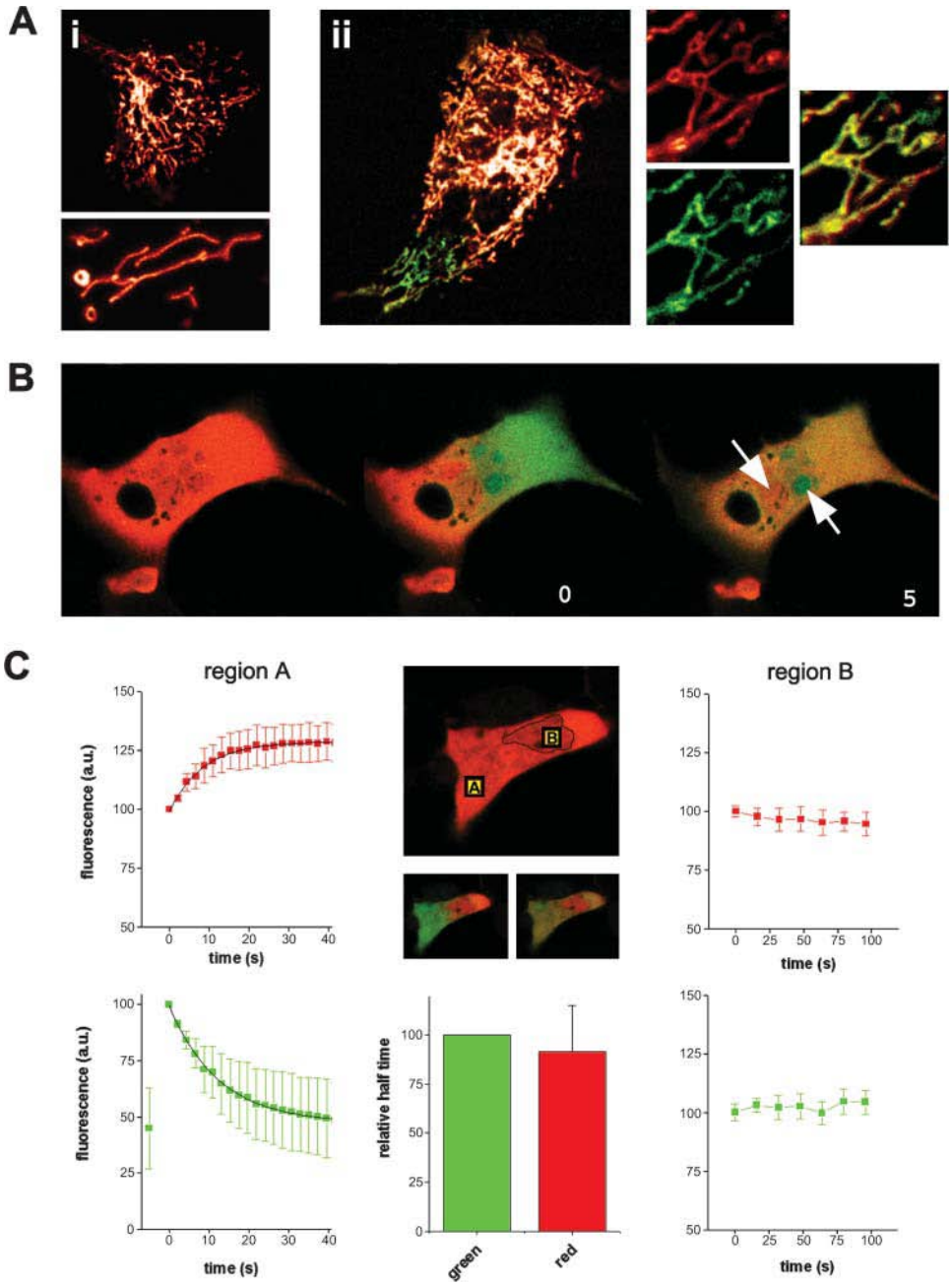

FIGURE 6 Subcellular labeling applications using DsRed-derived variants. (*A*) (*i*) *Top,* confocal images of HT-1080 cells expressing mitochondrially-targeted DsRed[N42Q]. *Bottom,* targeting of DsRed[N42Q] to mitochondria does not disrupt mitochondrial morphology. (*ii*) Greening of discrete subcellular regions of mitochondria in a HT-1080 cell expressing mitochondrially-targeted DsRed[N42Q]. *Far right,* higher magnification images of mitochondria before and after three-photon bleaching to illustrate the lack of effect of greening on mitochondrial morphology (*overlay*). (*B*) Confocal image sequence (λ_{EX} = 488 nm) of a DsRed-T3 expressing HT-1080 cell before (*left*) and after ($t = 0$; *middle*) exposure of the right-hand side of the cell to femtosecond irradiation ($\lambda_{EX} = 750$ nm). (*Right*) Image captured ~5 min later, showing equilibration of the color gradient by diffusional mixing throughout the cytoplasm, but not within the nucleus (*arrows*). (*C*) Cumulative measurements from DsRed[N42Q]-expressing HEK-293 cells showing average fluorescence intensities (*red squares*, $\lambda_{EM} > 585$ nm; *green squares*, $\lambda_{EM} = 522 \pm 17$ nm, normalized to value at $t = 0$) within regions A (areas of cytoplasm exposed to multiphoton beam) and B (intranuclear regions) before and after ($t = 0$) greening a region of cytoplasm. (*Right*) Example of depicted regions within a cell before multiphoton greening. Error bars reflect parallel measurements in different cells. The smaller images span the duration of a typical experiment after multiphoton greening. The bar graph compares the half-times of diffusion of the green and red species by curve-fitting the relaxation kinetics after multiphoton greening, and suggests that the green- and red-emitting species are of similar size.

lower aggregatory propensity of several variants, which likely increases cellular tolerance. However, improved maturation speed and/or improved folding may also be a key factor—for example, DsRed[N42Q] is considerably brighter than DsRed despite lacking the suite of NH_2-terminal substitutions which reduce aggregation (Fig. 1 *C ii*).

Second, to optimize the extent of the color change evoked by three-photon excitation, one would want to maximize the number of tetramers in which efficient FRET is occurring. FRET efficiency will be enhanced by mutations that directly impact protein structure to optimize energy transfer between donor and acceptor chromophores. Alternatively, the number of spectral (cf, anisotropic) FRET partners will be maximized by optimizing the heteromery of the DsRed population and mutations that vary the completeness of green chromophore maturation will impact the ratio of red to green monomers in the DsRed population. The crystallographic structure of DsRed suggests that FRET occurs most efficiently within the two antiparallel pairs of chromophores within the DsRed tetramer (Wall et al., 2000), suggesting that a red/green monomer ratio of unity would maximize the number of R_2G_2 species and thereby

the color change observed on greening. However, spectroscopic investigations of the composition of DsRed tetramers have demonstrated that the ratio of the red to green species is ~1.2–1.5, i.e., ~220–240 red monomers in 100 tetramers (Garcia-Parajo et al., 2001). Assuming the composition of tetramers is stochastically determined (Garcia-Parajo et al., 2001), mutations that drive the ratio of red to green species toward unity merit investigation as improved highlighter probes, even though these variants would exhibit increased green emission from the larger green homotetramer population relative to DsRed. Conversely, mutations that increase FRET efficiency likely decrease ''escaping'' green emission, especially if FRET can occur between chromophore pairs (Cotlet et al., 2001). Therefore, since FRET-optimizing mutations may be associated with increases or decreases in the magnitude of green fluorescence in the emission spectrum, we were receptive to screening variants with both higher (DsRed[N42Q], DsRed-2) and lower (DsRed-T1) green emission in this study relative to the DsRed-1.

Finally, the more practical issues of ease of evoking and monitoring the color change are important for experimentalists. We demonstrate here that the color change can just as easily be resolved with the argon-ion laser line ($\lambda_{EX} = 488$ nm) commonly found on laser-scanning instruments such as confocal microscopes and flow cytometers as well as with a standard FITC filter cube (Fig. 3 *C*). Although the method necessitates multiphoton excitation, it occurs rapidly (in a few seconds) and with the high spatial focality of three-photon excitation resulting in a color change that is spatially defined and easily visible by camera, photomultiplier tube, or eye.

N42Q and DsRed2 as improved optical highlighters.

Fig. 7 summarizes the properties of each RFP variant as an optical highlighter in terms of the extent of the color shift observed (Fig. 7 *A*), the properties of the probe in vitro and in vivo (Fig. 7 *B*), as well as the ease of evoking the color change (*bleaching rate*, Fig. 7 *B*). These data show that DsRed[N42Q] and DsRed-2 represent considerable improvements on DsRed in all these parameters—1), the intensity of the greened probe was brighter (Figs. 1 *C* and 7 *B*); 2), the average extent of the color change was greater (Figs. 2 *B* and 7 *A*); and 3), the color change was effected by shorter exposures to femtosecond irradiation. Consistently, cells expressing these variants exhibited a bright, vivid green coloration after multiphoton bleaching (Fig. 4). In contrast, DsRed-T1 had little utility as an optical highlighter, despite possessing the desirable properties of faster maturation, lower aggregation, and a more intense fluorescence expression in mammalian cells. For DsRed-T1, the multiphoton bleaching event was relatively incomplete such that residual red fluorescence masked the increase in green fluorescence, which often photobleached significantly during the longer exposure times required. The net result was cells of a dim yellow-orange appearance (Fig. 4). DsRed-T3 largely mimicked results with DsRed-T1, although occasional batches of transfected cells exhibited an adequate greening response despite the use of identical experimental protocols. We speculate that in these cases, the completeness of the in vivo maturation process was less such that the twofold enhancement of green fluorescence was more obvious. Factors that affect the completeness of the rate of chromophore

A

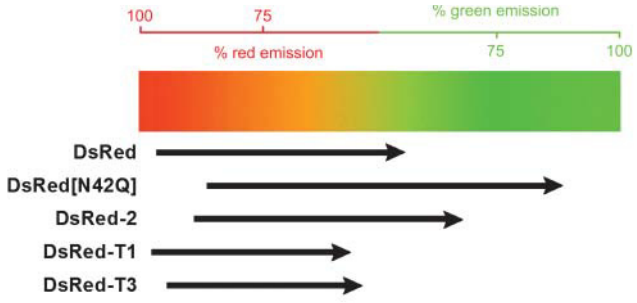

B

		DsRed	DsRed[N42Q]	DsRed-2	DsRed-T1	DsRed-T3	n≥
Cell Biology	aggregatory tendency	+	+				
	relative brightness *in vivo*	1	***1.68±0.12***	***2.28±0.29***	1.25±0.17	2.13±0.23	4
Biophysical Properties	excitation / emission max. (nm)	558 / 583	562 / 589	560 / 583	556 / 581	560 / 588	8
	quantum yield	0.69	0.62	0.47	0.55	0.68	3
	extinction coefficient ($M^{-1}cm^{-1}$)	57,000	32,000	43,800	28,300	53,900	
	relative brightness *in vitro*	***1.00***	***0.50***	***0.52***	***0.40***	***0.93***	
	green:red fluorescence (48hrs)	3.3 ± 1.4%	13.8 ± 2.1%	11.1 ± 2.0%	2.2 ± 0.5%	5.5 ± 1.4%	17
	power coefficient (excitation, λ=750nm)	1.68±0.19	1.64±0.29	1.65±0.12	1.59±0.22	1.63±0.14	4
	power coefficient (bleaching, λ=750nm)	2.98±0.10	3.05±0.57	2.69±0.16	n.d.	n.d.	3
	bleaching rate (normalized half-time)	1	***0.72±0.07***	***0.68±0.11***	1.14±0.23	1.31±0.29	4

FIGURE 7 Summary of results indicating suitability of different RFP variants as 'optical highlighters'. (*A*) Graphic illustrating the average extent of the color change observed for all five RFP variants induced by short-wavelength multiphoton excitation. The proportion of green to red fluorescence (peak green/peak red) in the emission spectrum before and after multiphoton bleaching of the red fluorophore defines the position of each arrow. (*B*) Table comparing the features of the DsRed-derived constructs measured from HEK-293 cells expressing individual variants, assessed using a spectrometer (emission maximum, red/green fluorescence ratio) by flow cytometry (relative brightness) and by multiphoton imaging (power coefficients, bleaching). Spectroscopic measurements of quantum yield and extinction coefficient were determined de novo from samples of DsRed[N42Q], DsRed-T1, and DsRed-T3 purified from bacteria, as described in Materials and Methods.

maturation remain poorly understood (Bevis and Glick, 2002; Terskikh et al., 2002), and we are investigating these considerations in a variety of different cell types. Our original impetus to investigate DsRed-T1 and DsRed-T3 derived from the observation that both these variants exhibit a pronounced green excitation shoulder (475–486 nm) but weak green emission (Bevis and Glick, 2002), possibly indicative of higher FRET efficiency. However, it is worth noting that the FRET efficiency between the green and red species of DsRed is already high (63–83% (Baird et al., 2000)), surpassing that of most constructs based on linkage of GFP variants, such that it may prove challenging to generate variants with marked improvements in this property. Certainly, the magnitude of the green fluorescence increase observed for DsRed-T3 (~2.2-fold) was no improvement over DsRed (~2.8-fold), and was significantly masked by the resistance of the red fluorophore to bleaching. The enhancement of green emission on multiphoton excitation was greater for DsRed-T1 (~4-fold) than DsRed, but again this change was masked by residual red fluorescence. Further, the large discrepancy in the absorption and excitation spectra for the DsRed-T1 green species (as with mRFP-1 (Campbell et al., 2002)), is suggestive of a poor average quantum yield for the green species, which is not an ideal property for a probe used for fluorescence imaging.

The mechanism by which three-photon excitation rapidly and selectively bleaches the red-emitting species remains to be defined. Three-photon excitation at $\lambda = 750$ nm nominally corresponds to one photon excitation at $\lambda = 250$ nm, within the barrel absorption. However, it is often the case that multiphoton excitation is considerably blue-shifted relative to the multiple of the one-photon excitation peak (Xu, 2000) and therefore the one-photon excitation peak ($\lambda = 330$ nm) displayed exclusively by the red but not the green form of DsRed variants may be relevant to this effect (Marchant et al., 2001). Further, it is noteworthy that both DsRed-2 and DsRed[N42Q] lack several amino acid substitutions shared between the later designed RFP variants with increased resistance to photobleaching (DsRed-T1, DsRed-T3, and mRFP-1). These include an NH_2-terminal mutation (N6D), two mutations external to the β-barrel (T21S, H41T), and two mutations internal to the β-barrel (V44A is localized within the plane of the chromophore, and T217A beneath). Both V44A and T217A, first introduced in DsRed-T1 (Bevis and Glick, 2002), have pronounced effects on the fluorescent properties of variants that harbor them (Bevis and Glick, 2002; Campbell et al., 2002) and may therefore influence the chromophore stability to multiphoton excitation. Our data (Fig. 5), as well as results from other groups strongly favor a FRET-dequenching mechanism underpinning the red-green color change (Baird et al., 2000; Cotlet et al., 2001; Garcia-Parajo et al., 2001; Gross et al., 2000; Lounis et al., 2001; Marchant et al., 2001; Wall et al., 2000; Yarbrough et al., 2001). Indeed, intratetrameric energy transfer has been detected for wild-type DsRed in single-molecule studies (Cotlet et al., 2001; Garcia-Parajo et al., 2001). Further, the observation that the emission and excitation spectra (Figs. 1 *B* and 4 *B*) of the enhanced green fluorescence species closely resembles that of the immature form, further suggests that a dequenching of preexisting green species underpins this phenomenon. However, despite the bulk of experimental evidence favoring FRET dequenching, many aspects of the photophysics of the DsRed molecule are still controversial (Campbell et al., 2002; Verkhusha et al., 2004), and we stress it remains possible that the color change may result from an as yet unidentified photoconversion mechanism (albeit to a green species with identical fluorescent properties to the immature form).

Why then are DsRed[N42Q] and DsRed-2—variants displaying elevated initial green fluorescence emission—more viable as optical highlighters? First, the ultimate intensity of the probe is determined by the amplitude of the green emission peak after comprehensive bleaching of red fluorescence. Since initial red fluorescence emission so dominates the basal green emission, there is sufficient leeway to trade red intensity for a higher level of initial green emission to maximize the visibility of the ultimate color change. Second, it is important to realize that increased basal green emission does not necessarily come at too high a price in terms of decreased intratetrameric FRET. If the composition of tetramers is stochastically determined (Garcia-Parajo et al., 2001), the number of R_2G_2 species is largely insensitive over wide variations in the red/green monomer ratio. For example, variation of the ratio of red to green species between 0.6 and 1.6 (150–250 red monomers per 100 tetramers) results in only an ~12% fluctuation in the number of R_2G_2 species but an ~800% change in the balance between R_4 and G_4 homotetramers. Therefore, variants such as DsRed[N42Q] can exhibit increased green homomer fluorescence emission, without an appreciable decline in the number of R_2G_2 tetramers and thereby the magnitude of the FRET change on multiphoton excitation (~2.7-fold). In contrast, DsRed-2 exhibited a considerably smaller increase in green emission (~1.3-fold) such that the mechanism of optical marking more resembled a direct photobleaching mechanism (Dunn et al., 2002) than a photobleaching associated with a significant enhancement of fluorescence from a dequenched FRET donor. Despite this lower change in green signal, cells expressing DsRed-2 were the brightest of all variants tested (Fig. 1 *C ii*; BD Biosciences Clontech 2001) and the comparatively complete and rapid bleaching of the red fluorescent species resulted in a viable probe where the level of green fluorescence emission dominated the small level of residual red emission (Fig. 4).

In conclusion, we have identified two red fluorescent protein variants, DsRed-2 and DsRed[N42Q], with improved properties over DsRed as optical highlighter tools. These probes complement the expanding biophotonic arsenal of

photolabeling tools and are well suited for live cell studies of fusion protein dynamics or optical tracking applications in mammalian cells.

SUPPLEMENTARY MATERIAL

An online supplement to this article can be found by visiting BJ Online at http://www.biophysj.org.

We thank Benjamin Glick (University of Chicago; DsRed[N42Q], DsRed-T3) and Roger Tsien (University of California, San Diego; mRFP-1) for their generous gifts of plasmids encoding RFPs.

This work was supported by a CAREER Fellowship Grant from the National Science Foundation (0237946).

REFERENCES

Ando, R., H. Hama, M. Yamamoto-Hino, H. Mizuno, and A. Miyawaki. 2002. An optical marker based on the UV-induced green-to-red photoconversion of a fluorescent protein. *Proc. Natl. Acad. Sci. USA*. 99: 12651–12656.

Baird, G. S., D. A. Zacharias, and R. Y. Tsien. 2000. Biochemistry, mutagenesis, and oligomerization of DsRed, a red fluorescent protein from coral. *Proc. Natl. Acad. Sci. USA*. 97:11984–11989.

BD Biosciences Clontech.2001. Living Colors DsRed2. *CLONTECHniques*. XVI:2–3.

Bevis, B. J., and B. S. Glick. 2002. Rapidly maturing variants of the *Discosoma* red fluorescent protein (DsRed). *Nat. Biotechnol.* 20:83–87.

Campbell, R. E., O. Tour, A. E. Palmer, P. A. Steinbach, G. S. Baird, D. A. Zacharias, and R. Y. Tsien. 2002. A monomeric red fluorescent protein. *Proc. Natl. Acad. Sci. USA*. 99:7877–7882.

Chudakov, D. M., V. V. Belousov, A. G. Zaraisky, V. V. Novoselov, D. B. Staroverov, D. B. Zorov, S. Lukyanov, and K. A. Lukyanov. 2003. Kindling fluorescent proteins for precise in vivo photolabeling. *Nat. Biotechnol.* 21:191–194.

Cotlet, M., J. Hofkens, S. Habuchi, G. Dirix, M. A. Guyse, J. Michiels, J. Vanderleyden, and F. C. D. Schryver. 2001. Identification of different emitting species in the red fluorescent protein DsRed by means of ensemble and single-molecule spectroscopy. *Proc. Natl. Acad. Sci. USA*. 98:14398–14403.

Dunn, G. A., I. M. Dobbie, J. Monypenny, M. R. Holt, and D. Zicha. 2002. Fluorescence localization after photobleaching (FLAP): a new method for studying protein dynamics in living cells. *J. Microsc.* 205:109–112.

Garcia-Parajo, M. F., M. Koopman, E. M. P. H. van Dijk, V. Subramanian, and N. F. van Hulst. 2001. The nature of fluorescence emission in the red fluorescent protein DsRed, revealed by single-molecule detection. *Proc. Natl. Acad. Sci. USA*. 98:14392–14397.

Gross, L. A., G. S. Baird, R. C. Hoffman, K. K. Baldridge, and R. Y. Tsien. 2000. The structure of the chromophore within DsRed,a red fluorescent protein from coral. *Proc. Natl. Acad. Sci. USA*. 97:11990–11995.

Gurskaya, N. G., A. V. Fradkov, A. Terskikh, M. V. Matz, Y. A. Labas, V. I. Martynov, Y. G. Yanushevich, K. A. Lukyanov, and S. A. Lukyanov. 2001. GFP-like chromoproteins as a source of far-red fluorescent proteins. *FEBS Lett.* 507:16–20.

Hadjantonakis, A. K., M. E. Dickinson, S. E. Fraser, and V. E. Papaioannou. 2003. Technicolor transgenics: imaging tools for functional genomics in the mouse. *Nat. Rev. Genet.* 4:613–625.

Heikal, A. A., S. T. Hess, G. S. Baird, R. Y. Tsien, and W. W. Webb. 2000. Molecular spectroscopy and dynamics of intrinsically fluorescent proteins: coral red (dsRed) and yellow (Citrine). *Proc. Natl. Acad. Sci. USA*. 97:11996–12001.

Hess, S. T., E. D. Sheets, A. Wagenknecht-Wiesner, and A. A. Heikal. 2003. Quantitative analysis of the fluorescence properties of intrinisically fluorescent proteins in living cells. *Biophys. J.* 85:2566–2580.

Jakobs, S., V. Subramaniam, A. Schonle, T. M. Jovin, and S. W. Hell. 2000. EGFP and DsRed expressing cultures of Escherichia coli imaged by confocal, two-photon, and fluorescence lifetime microscopy. *FEBS Lett.* 479:131–135.

Labas, Y. A., N. G. Gurskaya, Y. G. Yanushevich, A. F. Fradkov, K. A. Lukyanov, S. A. Lukyanov, and M. V. Matz. 2002. Diversity and evolution of the green fluorescent protein family. *Proc. Natl. Acad. Sci. USA*. 99:4256–4261.

Lippincott-Schwartz, J., N. Altan-Bonnet, and G. H. Patterson. 2003. Photobleaching and photoactivation: following protein dynamics in living cells. *Nat. Cell Biol.* 5:S7–S14.

Lippincott-Schwartz, J., E. Snapp, and A. Kenworthy. 2001. Studying protein dynamics in living cells. *Nat. Rev. Mol. Cell Biol.* 2:444–456.

Lounis, B., J. Deich, F. I. Rosell, S. G. Boxer, and W. E. Moerner. 2001. Photophysics of DsRed, a red fluorescent protein, from the ensemble to the single-molecule level. *J. Phys. Chem.* 105:5048–5054.

Marchant, J. S., G. E. Stutzmann, M. A. Leissring, M. A. LaFerla, and I. Parker. 2001. Multiphoton-evoked color change of DsRed as an optical highlighter for cellular and subcellular labeling. *Nat. Biotechnol.* 19: 645–649.

Marchant, J. S., V. S. Subramanian, I. Parker, and H. M. Said. 2002. Intracellular trafficking and membrane targeting mechanisms of the human reduced folate carrier in mammalian epithelial cells. *J. Biol. Chem.* 277:33325–33333.

Matz, M. V., A. F. Fradkov, Y. A. Labas, A. P. Savitsky, A. G. Zaraisky, M. L. Markelov, and S. A. Lukyanov. 1999. Fluorescent proteins from nonbioluminescent anthozoa species. *Nat. Biotechnol.* 17:969–973.

Matz, M. V., K. A. Lukyanov, and S. A. Lukyanov. 2002. Family of the green fluorescent protein: journey to the end of the rainbow. *Bioessays*. 24:953–959.

Miyawaki, A. 2002. Green fluorescent protein-like proteins in reef Anthozoa animals. *Cell Struct. Funct.* 27:343–347.

Mizuno, H., A. Sawano, P. Eli, H. Hama, and A. Miyawaki. 2001. Red fluorescent protein from Discosoma as a fusion tag and a partner for fluorescence resonance energy transfer. *Biochemistry.* 27:2502–2510.

Patterson, G. H., and J. Lippincott-Schwartz. 2002. A photoactivatable GFP for selective photolabeling of proteins and cells. *Science*. 297:1873–1877.

Salih, A., A. Larkum, G. Cox, M. Kuhl, and O. Hoegh-Guldberg. 2000. Fluorescent pigments in corals are photoprotective. *Nature*. 408:850–853.

Terskikh, A., A. Fradkov, G. Ermakova, A. Zaraisky, P. Tan, A. V. Kajava, X. Zhao, S. Lukyanov, M. Matz, S. Kim, I. Weissman, and P. Siebert. 2000. ''Fluorescent timer'': protein that changes color with time. *Science*. 290:1585–1588.

Terskikh, A. V., A. F. Fradkov, A. G. Zaraisky, A. V. Kajava, and B. Angres. 2002. Analysis of DsRed mutants. *J. Biol. Chem.* 277:7633–7636.

Verkhusha, V. V., D. M. Chudakov, N. G. Gurskaya, S. Lukyanov, and K. A. Lukyanov. 2004. Common pathway for the red chromophore formation in fluorescent proteins and chromoproteins. *Chem. Biol.* 11: 845–854.

Verkhusha, V. V., I. M. Kuznetsova, O. V. Stepanenko, A. G. Zaraisky, M. M. Shavlovsky, K. K. Turoverov, and V. N. Uversky. 2003. High stability of Discosoma DsRed as compared to Aequorea EGFP. *Biochemistry*. 42:7879–7884.

Verkhusha, V. V., and K. A. Lukyanov. 2004. The molecular properties and applications of Anthozoa fluorescent proteins and chromoproteins. *Nat. Biotechnol.* 22:289–296.

Verkhusha, V. V., H. Otsuna, T. Awasaki, H. Oda, S. Tsukita, and K. Ito. 2001. An enhanced mutant of red fluorescent protein DsRed for double labeling and developmental timer of neural fiber bundle formation. *J. Biol. Chem.* 276:29621–29624.

Wall, M. A., M. Socolich, and R. Ranganathan. 2000. The structural basis for red fluorescence in the tetrameric GFP homolog DsRed. *Nat. Struct. Biol.* 7:1133–1138.

Williams, A. T. R., S. A. Winfield, and J. N. Miller. 1983. Relative fluorescence quantum yield using a computer controlled luminescence spectrometer. *Analyst.* 108:1067–1071.

Xu, C. 1999. Two photon cross sections of indicators. *In* Imaging Living Cells. R. Yuste, F. Lanni, and A. Konnerth, editors. Cold Spring Harbor Laboratory Press, Woodbury, NY. Chapter 19.

Yanushevich, Y. G., D. B. Staroverov, A. P. Savitsky, A. F. Fradkov, N. G. Gurskaya, M. E. Bulina, K. A. Lukyanov, and S. A. Lukyanov. 2002. A strategy for the generation of non-aggregating mutants of *Anthozoa* fluorescent proteins. *FEBS Lett.* 511:11–14.

Yarbrough, D., R. M. Wachter, K. Kallio, M. V. Matz, and S. J. Remington. 2001. Refined crystal structure of DsRed, a red fluorescent protein from coral, at 2.0-A resolution. *Proc. Natl. Acad. Sci. USA.* 98:462–467.